Dually charged polyamide nanofiltration membranes fabricated by microwave-assisted grafting for heavy metals removal

Ben-Qing Huang [a,b], Yong-Jian Tang [a]*, An-Ran Gao [a], Zuo-Xiang Zeng [a], Shuang-Mei Xue [c], Chen-Hao Ji [c], Chuyang Y. Tang [d], Zhen-Liang Xu [a]*[1]

[a] *State Key Laboratory of Chemical Engineering, Membrane Science and Engineering R&D Lab, Chemical Engineering Research Center, School of Chemical Engineering, East China University of Science and Technology, 130 Meilong Road, Shanghai 200237, China*

[b] *Institute of Flow-Induced Corrosion and Intelligent Prevention and Control, Changzhou University, Changzhou 213000, China*

[c] *Institute for Advanced Study, Shenzhen University, Shenzhen 518060, China*

[d] *Department of Civil Engineering, The University of Hong Kong, Pokfulam HW619B, Hong Kong, China*

GRAPHIC ABSTRACT

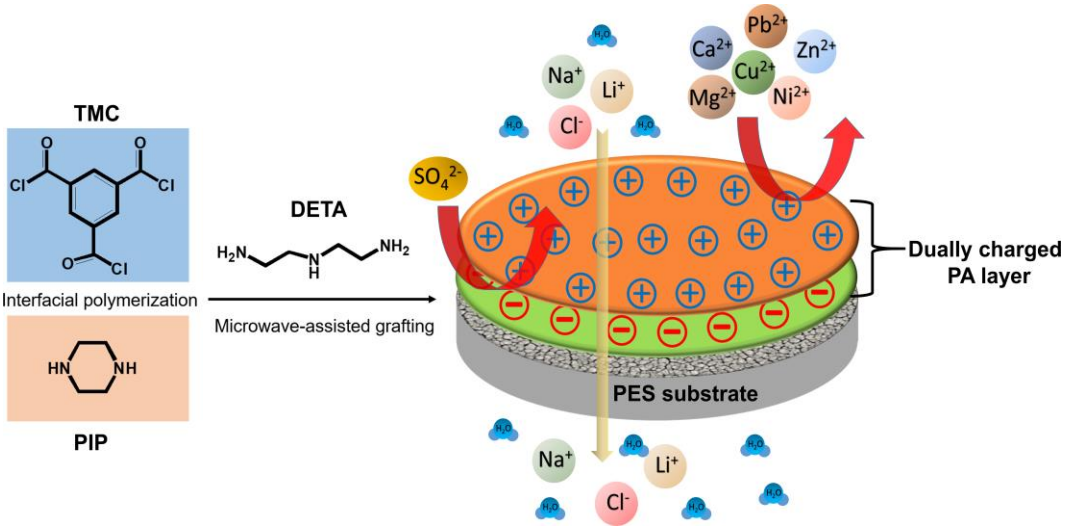

* To whom all correspondence should be addressed.
Email: tangyongjian@ecust.edu.cn, chemxuzl@ecust.edu.cn.

ABSTRACT: Heavy metals pollution is an urgent problem that seriously hazards human health and ecosystems. Herein, dually charged nanofiltration (NF) membranes were prepared via a facile modification with diethylenetriamine (DETA) after interfacial polymerization. More amine groups were imported after grafting and a polyamide layer with opposite charges was constructed. The as-prepared membranes had a pure water permeability of 17.0 L m^{-2} h^{-1} bar^{-1} and maintained ideal rejection for both Na_2SO_4 (98.2%) and $MgCl_2$ (94.1%), illustrating dually charged property. In addition, the dually charged NF membranes had high rejection to a series of heavy metals, showing good application potential in heavy metals removal.

Keywords: Nanofiltration, Grafting, Dually charged, Heavy metals

1. Introduction

Heavy metals, typically like copper, lead, zinc, nickel, chromium, cadmium, and mercury, have specific gravities of greater than or equal to 4.0 [1] and are often present in high concentrations in wastewater of mining, smelting, electroplating, and chemical industries [2, 3]. If released into the environment, heavy metals can potentially pose huge threats to the ecosystem and human health [4]. Many heavy metals can bind to proteins and destroy their enzymatic activities, thus affecting biological/physiological activities and leading to chronic poisoning and even death [5]. Commonly methods of heavy metal removal from contaminated water include adsorption, chemical precipitation, ion exchange, and electrodeposition. Nevertheless, these methods often suffer deficiencies such as high cost in equipment and operation, low removal rate, detrimental metal sludge [6]. Therefore, developing new alternative technology is imperative.

Nanofiltration (NF) is a pressure-driven membrane technology increasingly used for wastewater treatment [7-9]. It separates solutes from water mainly through size sieving and electrostatic interaction. With suitable pore size and tailorable surface charge property, NF technology shows superiorities in separating small-molecular-weight pollutants and salts with characteristics of high efficiency, low expense, no chemical or thermal addition, and environmentally friendliness [10].

Surface charge plays a decisive role in ion sieving performance [11]. The commonly commercial NF membranes are polyamide (PA) membranes fabricated via interfacial polymerization (IP). The typical PA NF membranes, using piperazine (PIP) and trimesoyl chloride (TMC) for IP, are generally negatively charged and show high rejection to multivalent anions while low rejection to monovalent anions, thus offering selective removal of the former [12, 13]. On the other hand, the negatively charged NF membranes tend to have unsatisfactory performance in separating cations. For example, the commercial PA NF membrane NF270 only has a $CaCl_2$ rejection of 40-60% [9]. Positively charged NF membranes have been developed to achieve enhanced cation separation [14, 15]. The PA NF membranes prepared by IP with polyethyleneimine (PEI) and TMC were positively charged, showing good Mg^{2+}/Li^{+} separating performance [16]. But the positively charged NF membranes usually sacrifice anion separation ability [17]. Therefore, the NF membranes with a single charge (negatively or positively) cannot achieve the requirement of purifying wastewater with complex composition of ions [18].

Dually charged NF membranes, having high divalent cations rejections and high divalent anions rejections concurrently, have become a new research category in the field of NF technology, and have a broad application prospect. The key to fabricating dually charged NF membranes is constructing oppositely charged separating layers. Alternative deposition of oppositely charged molecules on the substrate is a commonly used method to fabricate dually charged composite membranes [19, 20]. The charges and thickness could be adjusted expediently by the co-deposition times [21]. Fewer co-deposition times usually leads to a loose membrane structure that cannot meet the separation requirements [22]. Increasing co-deposition times makes the preparation process more complicated, and increases the operating cost accordingly. Controlling the amount of monomers involved in the IP process is also a common method to prepare dually charged NF membranes [23, 24]. The PA layer with opposite charges can be generated in a single IP process. Even though, the requirement of accurate control on fabricating parameters is high and increases the

industrialization difficulties. Thus, developing a simple and effective preparation method of dually charged NF membranes is of great impendency.

Herein, a facile strategy to fabricate dually charged NF membranes based on the IP process was presented. The commonly negatively charged PA membrane prepared by IP with PIP and TMC was modified by diethylenetriamine (DETA) to construct an oppositely charged PA NF membrane. The differences in chemical structure, micromorphology, hydrophilicity, and charge of the fabricated NF membranes before and after grafting were characterized in detail. A series of experiments were conducted to evaluate separation ability. The potential for heavy metals removal of the fabricated dually charged NF membranes were also evaluated.

2. Experimental section

2.1 Chemicals and materials

Polyether sulfone ultrafiltration (PES UF) membranes, used as substrates for IP, were provided by Hangzhou Water Treatment R&D Center (China), which molecular weight cutoff (MWCO) was 50,000 Da. Piperazine (PIP, 99.5%) was provided by J&K Scientific Co., Ltd. (China). Trimesoyl chloride (TMC, 98%) and diethylenetriamine (DETA, 99%) were provided by Aladdin Bio-Chem Technology Co., Ltd. (China). Inorganic salts (Na_2SO_4, $MgSO_4$, Li_2SO_4, $NiSO_4$, $ZnSO_4$, $CuSO_4$, $MgCl_2$, NaCl, $CaCl_2$, LiCl, $Cu(NO_3)_2$, and $Pb(NO_3)_2$, AR), organic solvent (n-hexane, AR), polyethylene glycol (PEG, CP), and high-purity KCl (≥99.9%) were provided by Sinopharm Chemical Reagent Co., Ltd. (China).

2.2. Fabrication of NF membranes

Before preparation, PES UF substrates were completely immersed with DI water for at least 48 hours to remove the impurities thoroughly. Organic solution with 0.1 wt% TMC (n-hexane as solvent), aqueous solution with 0.1 wt% PIP, and aqueous solutions with DETA concentrations of 0.005~0.05 wt% were prepared and ultrasonicated for 30 min. Firstly, the PES UF membrane was suspended vertically and air-dried to remove water drops from its surface. Then the membrane was fixed with Teflon frames to make sure that the chemicals only contacted with the upside of

the membrane in the subsequent operation. Secondly, the PIP solution (25 mL) was poured in the frames and immersed the top-surface. After contact of 3 minutes, this PIP solution was poured away, and the residual water drops were swept away with compressed air with 0.2 MPa. Next, 25 mL TMC solution was poured onto the membranes and removed 15 s later. Then the membranes were immersed with 25 mL DETA solution and contacted for 60 s. At last, the membrane was heat-treated using microwave (**Fig. S1**) for 1 min. The label of membrane sample was MDX where X represented the concentration of DETA (wt%), with the blank membrane without DETA grafting denoted as M0 (The preparation parameters of membranes were listed in **Table S2** in detail). The preparation process of NF membranes and possible reactions are shown in **Fig. 1**. All the prepared membranes were kept in DI water to remove unreacted chemicals until further tests and analysis.

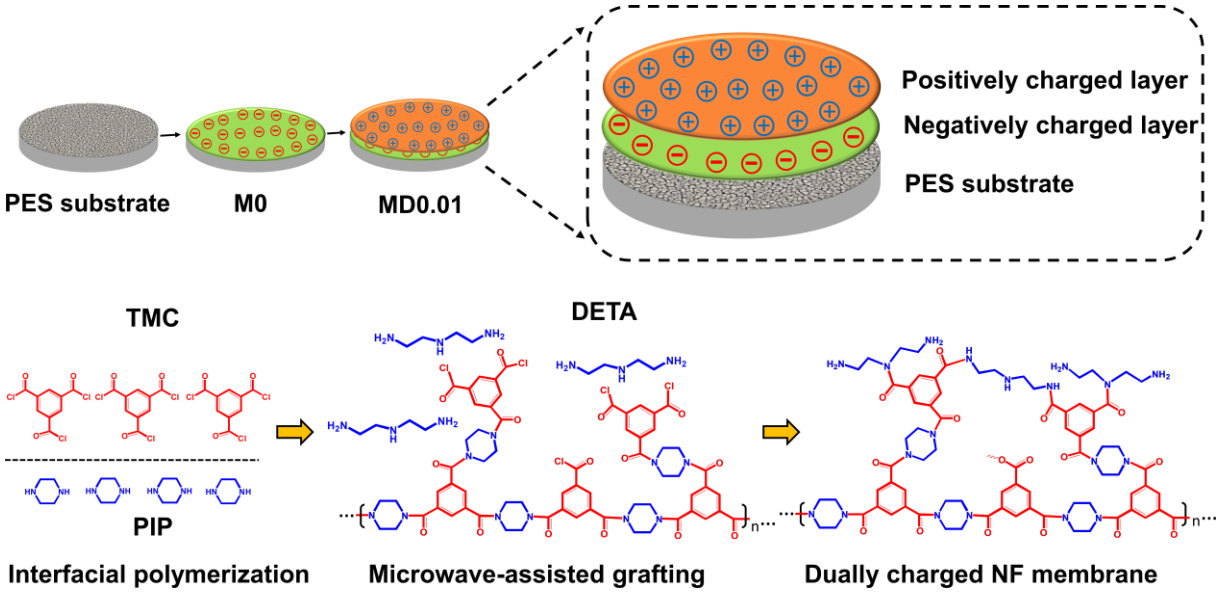

Fig. 1. Diagram and possible reactions of IP and DETA grafting process.

2.3. Characterization

A Fourier transform infrared spectrometer (FTIR, Magna-IR550, Nicolet, USA) with an attenuated total reflection (ATR) accessory and an X-ray photoelectron spectrometer (XPS, K-Alpha, Thermo Fisher, USA) with Al Kα radiation (hv=1486.6 eV) as the X-ray source and a hemispherical energy analyzer was used to analyze chemical composition. The pass energy and resolution were 100 eV and 1 eV for wide scan mode and 50 eV and 0.05 eV for high resolution mode. A scanning electron

microscope (SEM, Nova Nano450, FEI, USA) with the electron energy of 3 kV and a Helix detector was applied to observe micromorphology with a magnification of 50,000. An atomic force microscope (AFM, Multi 8, Bruker, Germany) was used to analyze roughness and the testing area was 5 μm×5 μm. A contact angle meter (JC2000D, Powereach, China) was applied to test pure water contact angle (WCA). A streaming potential analyzer (SurPASS, Anton Paar, Austria) was used to evaluate the charge property with 0.01 mol L^{-1} KCl which pH was adjusted by 0.05 mol L^{-1} KOH and HCl.

2.4. NF performance test

The as prepared NF membranes were tested using a lab-scale device with three identical crossflow test cells. The tested membranes were circular with a diameter of 6.0 cm. Before testing, the device maintained stable operation under 5.0 bar for 30 min.

The pure water permeability (PWP) was calculated with Eq. 1:

$$PWP = \frac{V}{A \cdot t \cdot P} \quad (1)$$

where V was the volume of permeating solution (L) with collecting time of t (h), A and P were the permeating area (m^2) and pressure (bar).

The rejection was calculated with Eq. 2:

$$R = \left(1 - \frac{C_P}{C_F}\right) \times 100\% \quad (2)$$

where C_P and C_F were the concentrations of solute in permeation and feed.

The salts concentrations were detected using a conductivity meter (DDS-11A, INESA, China). The concentrations of PEGs were measured by a total organic carbon analyzer (TOC, TOCVPN, Shimadzu, Japan). The concentrations of heavy metals were tested with an atomic absorption spectrometer (4510F, INESA, China).

3. Results and discussion

3.1 Surface composition

Fig. 2 shows the FTIR spectra. The peaks of 1440 cm^{-1} and 3400 cm^{-1} were assigned to N-H in-plane bending and O-H stretching vibration [25]. The peak appearing at 1652 cm^{-1}corresponded to the C=O stretching vibration of the amide

bond [26]. The FTIR results illustrates the formation of polyamide. The chemical composition of the membranes was analyzed using XPS. **Fig. 3** and **Table 1** show the XPS spectra and elemental composition of PES UF substrate, M0, MD0.005, and MD0.01. 4.7 % sulfur element (168.0 eV) was detected in PES substrate. After the IP process, the three NF membranes showed a new nitrogen peak (400.0 eV) but no sulfur peak. It confirms that a PA layer had been formed through the IP reaction and fully covered the substrate [27]. The N/O ratio of M0 is 0.72. Grafting DETA led to increased N/O ratios (0.79 for MD0.005 and 0.85 for MD0.01). Consistently, the deconvoluted peaks of C 1s of high resolution XPS spectra (**Fig. 3b-d**) had the greater percentage of C-N after grafting, which is attributed to the successful grafting of DETA onto the membrane surface [28, 29]. The XPS results demonstrated a positively charged layer had been successfully built after the grafting of DETA which can strengthen the rejection to divalent cations of the membranes. In addition, the percentage of N-C=O was increasing with the grafting, which indicated the greater crosslinking degree of membranes [28]. The N 1s spectra in **Fig. S3** also illustrates the increment of N-C=O percentages. The membranes with higher crosslinking degree had smaller pore size which increased rejection to organics but sacrificed permeability.

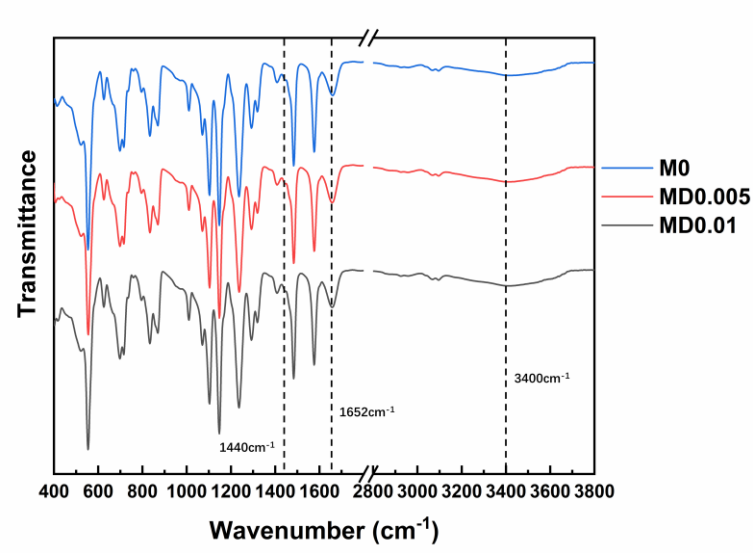

Fig. 2. FTIR spectra of NF membranes.

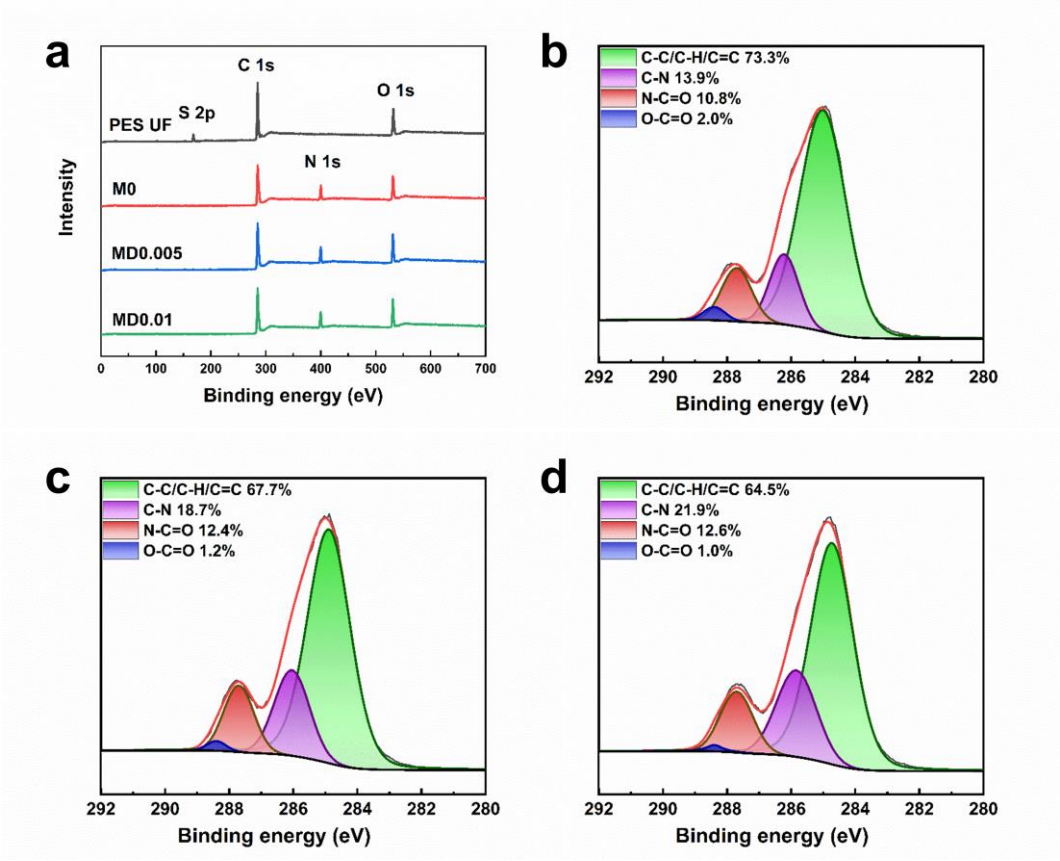

Fig. 3. (a) XPS spectra of PES UF substrate, M0, MD0.005, and MD0.01. C 1s spectra of (b) M0, (c) MD0.005, and (d) MD0.01.

Table 1 Elemental composition of PES UF substrate, M0, MD0.005, and MD0.01.

Sample	Atomic percent (%)				N/O ratio
	C 1s	N 1s	O 1s	S 2p	
PES UF	76.7±0.7	/	18.6±0.4	4.7±0.3	/
M0	71.1±1.0	12.1±0.5	16.8±0.5	/	0.72±0.05
MD0.005	69.5±0.9	13.5±0.4	17.0±0.4	/	0.79±0.04
MD0.01	69.8±1.1	13.9±0.5	16.3±0.4	/	0.85±0.05

3.2. Membrane morphology

SEM and AFM are commonly used and effective way to analyze morphology. **Fig. 4a-d** show the top-surface images of PES substrate, M0, MD0.005, MD0.01, and **e-h** are the corresponding cross-section images. The surface of the PES UF membrane and M0 (the typical polypiperazine-amide membrane) was relatively smooth, which is consistent with previous work [12]. After DETA grafting, circular protuberances can be observed on the membrane surface. Similar morphology had been observed on NF membranes prepared by grafting [27]. The unbalance in interfacial tension during the grafting leads to the shrinkage of the PA layer. **Fig. 5** shows the AFM images and roughness of the UF substrate and NF membranes. The surface morphology and roughness results Ra and Rms (mean surface roughness and root mean square roughness) obtained by AFM were consistent with the SEM characterization.

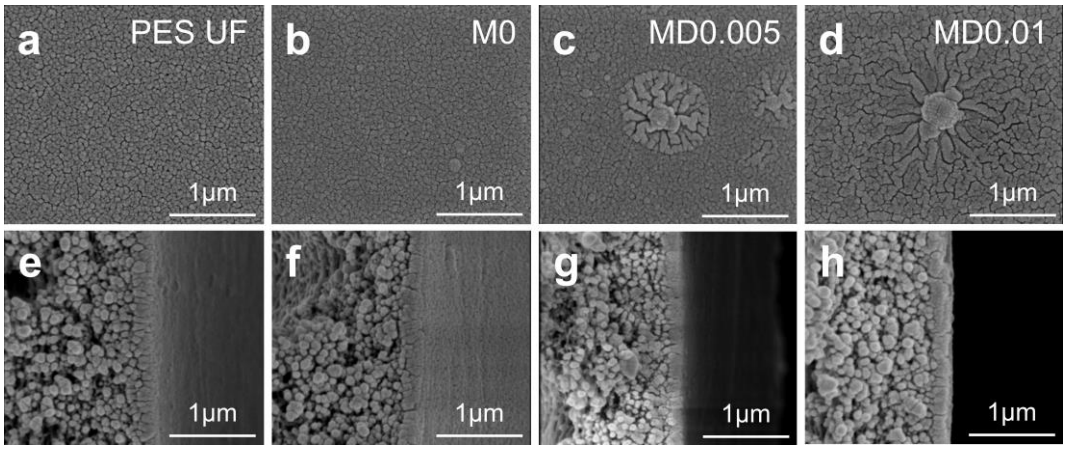

Fig. 4. SEM images of (a and e) PES UF substrate, (b and f) M0, (c and g) MD0.005, and (d and h) MD0.01.

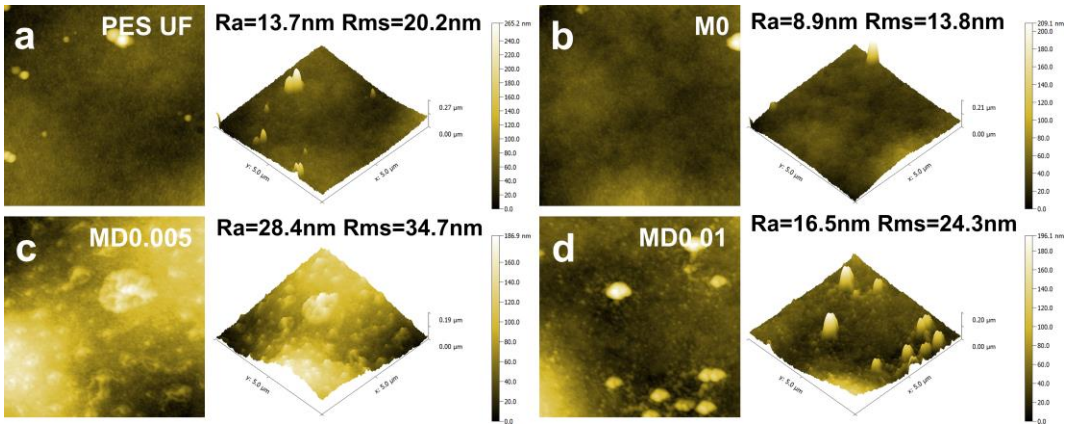

Fig. 5. AFM results of (a) PES UF substrate, (b) M0, (c) MD0.005, and (d) MD0.01 (testing area of 5μm×5μm).

3.3. Surface properties

Hydrophilicity and charge are the important surface properties that are closely related to the permeability, ion selectivity, and antifouling performance of NF membranes [30-32]. WCA and zeta potential are the commonly used methods to represent the hydrophilicity and charge, respectively [28, 33]. **Fig. 6a** shows the WCA of 0 s (measured at the moment of water drops contact with membrane surface) and after 120 s. The WCA decreased obviously from 0 s to 120 s because the water infiltrated with longer contact time [34]. All the PA NF membranes had better hydrophilicity than PES substrate on account of the difference of PES and PA in hydrophilicity [35]. The WCA of NF membranes with DETA grafting was smaller than M0. After grafting, more amine groups are introduced onto the membrane surface which enhances the hydrophilicity. In addition, the leaf-like venation increased the contact area with water, which tends to reduce the contact angle [36]. **Fig. 6b** shows the zeta potential of M0, MD0.005, and MD0.01 over a pH range of 4-10. With the test condition changing from acid to alkaline, the zeta potential decreased. The PA layer is positively charged with the amine groups protonated at low pH while negatively charged with amine and carboxylic acid groups deprotonated at high pH [37]. The isoelectric point (IEP) of M0, MD0.005, and MD0.01 were 3.84, 4.44, and 5.67. Generally speaking, higher IEP means that the membrane is more positively charged [38]. The DETA grafting introduces more amine groups to the

membrane surface, resulting in more positively charged surface and enhanced rejection to divalent cations of the membranes [39].

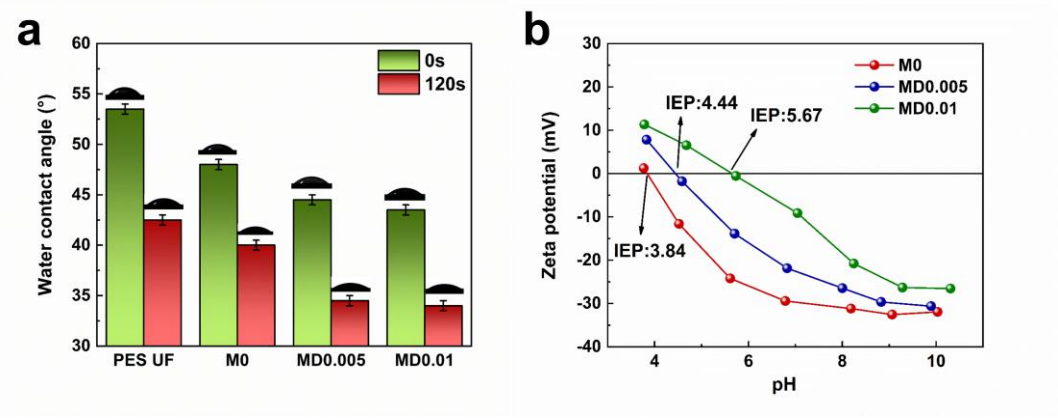

Fig. 6. (a) WCA of PES UF substrate, M0, MD0.005, and MD0.01. (b) Zeta potential of M0, MD0.005, and MD0.01 at pH value ranging of 4-10.

3.4. The effect of DETA concentration

The membranes were fabricated with different concentrations of DETA. The PWP and rejections to different salts were tested and shown in **Fig. 7**. After grafting, the PWP decreased from 31.4 (M0) to 18.7 L m^{-2} h^{-1} bar^{-1} (MD0.005). The DETA grafting makes PA layer further cross-linked according to the XPS results, thus the permeability decreases. With further increasing of DETA concentration, the PWP showed slight decline. M0 showed high rejection to Na_2SO_4, moderate rejection to $MgSO_4$, while low rejection to $MgCl_2$ and NaCl, which is typical for polypiperazine-amide membranes with a negatively charged PA separating layer. After DETA modification, the NF membranes maintained high rejection to Na_2SO_4. At the same time, the rejection of $MgSO_4$ increased to >96.5%. The $MgCl_2$ rejection also increased obviously (from 18.7% of M0 to 78.0% of MD0.005). With DETA concentration increasing to 0.01%, $MgCl_2$ rejection increased to 94.1%. Further increasing of DETA concentration had a negligible effect on $MgCl_2$ rejection. The grafting of DETA constructs a positively charged layer, thereby increasing the rejection of Mg^{2+}. **Fig. 8** shows the mechanism of the negatively and dually charged NF membranes for ions rejection. The negatively charged membranes like M0 only have a PA layer with a negative charge. Due to the Donnan effect, the divalent anions

can be resisted by the membrane but the divalent cations will transport across the membrane to a great extent [40]. The dually charged NF membranes have both a positively and negatively charged layer. The positively charged layer intercepts divalent cations while the negatively charged layer intercepts divalent anions, thus the membrane has good separating ability for both divalent cations and anions [18, 41].

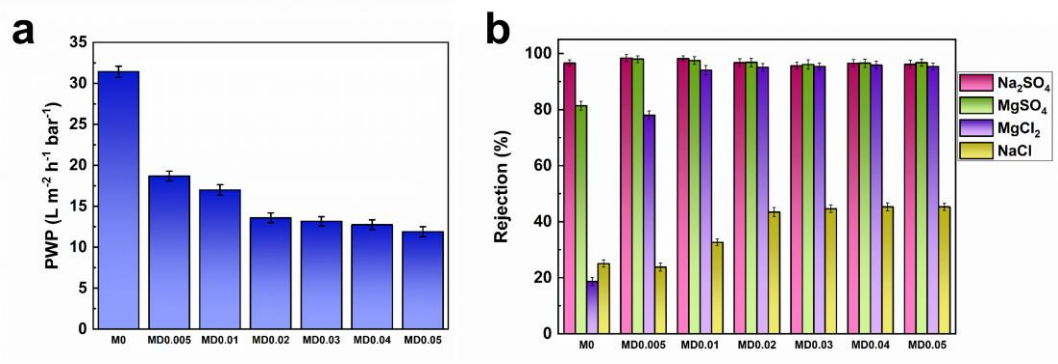

Fig. 7. (a) PWP and (b) Rejection to salts of M0 and membranes grafted with different concentrations of DETA (2000 ppm, 25 ℃, 5.0 bar).

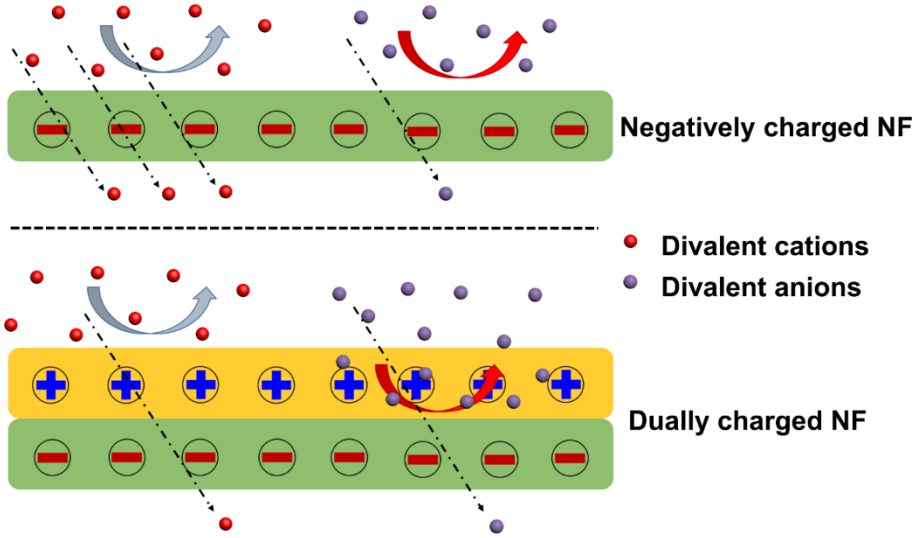

Fig. 8. Separation mechanism of the negatively and dually charged NF membranes.

3.5. NF performance

The permeability and rejection of MD0.01 to different salts were tested and shown in **Fig. 9a**. The rejection of MD0.01 to a series of inorganic salts was in the following order: Na_2SO_4 (98.2%) > $MgSO_4$ (97.5%) > Li_2SO_4 (96.3%) > $MgCl_2$ (94.1%) > $CaCl_2$ (82.6%) > LiCl (36.7%) > NaCl (32.7%). MD0.01 showed high rejection for divalent cations (Mg^{2+} and Ca^{2+}) and divalent anions (SO_4^{2-}) but low rejection to monovalent salts (LiCl and NaCl). Mg^{2+} has bigger hydrated radius than

Ca^{2+}, so the rejection of $MgCl_2$ is higher than $CaCl_2$ [42]. The salts rejection results reflect the dually charged characteristic of MD0.01. The rejection of NF membrane to different PEG is often used to assess its pore size [43]. **Fig. 9b** showed the rejection of M0, MD0.005, and MD0.01 to PEGs. The rejection of MD0.005 and MD0.01 was higher than M0. The DETA reacted with acyl chloride groups and made a more cross-linked polymer structure, causing tighter membrane pores and thus increased rejection. The rejection of 90% is generally defined as the MWCO of NF membranes [28, 44]. The MWCO of M0, MD0.005, and MD0.01 are 357, 283, and 212 Da, respectively. The pore size is consistent with the result of crosslinking degree analyzed by XPS.

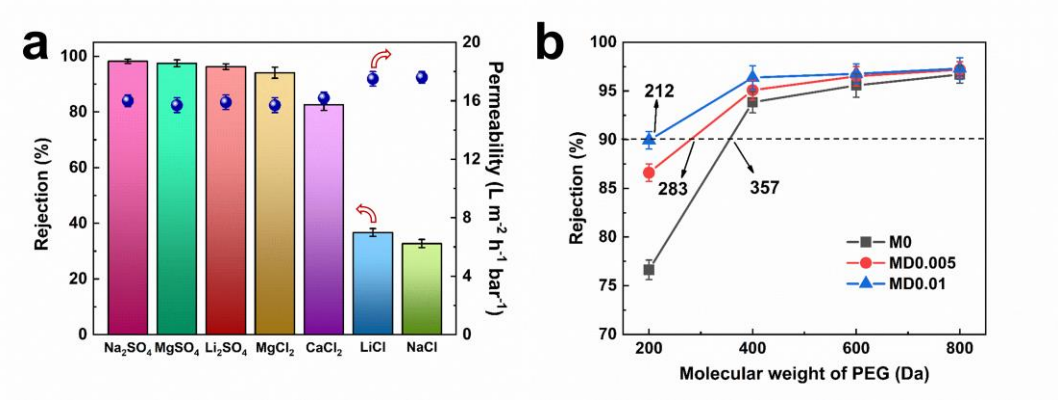

Fig. 9. (a) Rejection and permeability to different salts solution of MD0.01 (2000 ppm, 25 ℃, 5.0 bar). (b) Rejection to PEGs with different molecular weight of M0, MD0.005, and MD0.01 (300 ppm, 25 ℃, 5.0 bar).

3.6. Separation of heavy metals

The separation performance of M0 and MD0.01 to heavy metals was tested with 2000 ppm salts solutions. The rejection to 2000 ppm heavy metal are shown in **Fig. 10a**. M0 showed high rejection to $NiSO_4$(96.6%), $ZnSO_4$(96.8%), and $CuSO_4$(94.7%). The surface of M0 was negatively charged which had high rejection to divalent anions but low rejection to cations. So the rejection of $Cu(NO_3)_2$ and $Pb(NO_3)_2$ was low (53.2% and 44.7%, respectively). The rejection of MD0.01 to $NiSO_4$, $ZnSO_4$, $CuSO_4$, $Cu(NO_3)_2$, and $Pb(NO_3)_2$ were 94.8%, 94.5%, 92.9%, 89.0%, and 85.1%, respectively. The MD0.01 is dually charged, thus has high rejection to divalent cations, showing good separation performance for heavy metals. The long term test of MD0.01 with

different heavy metals were carried out and the results are shown in **Fig. 10b**. The rejection remained stable during the 7-day test, demonstrating the stability of MD0.01. **Fig. 10c** shows the PWP and rejection to heavy metals of MD0.01 and some NF membranes in literature. The detailed testing conditions were listed in **Table S4**. The dually charged MD0.01 has a high permeance and acceptable rejection to heavy metals compared with the NF membranes in literature.

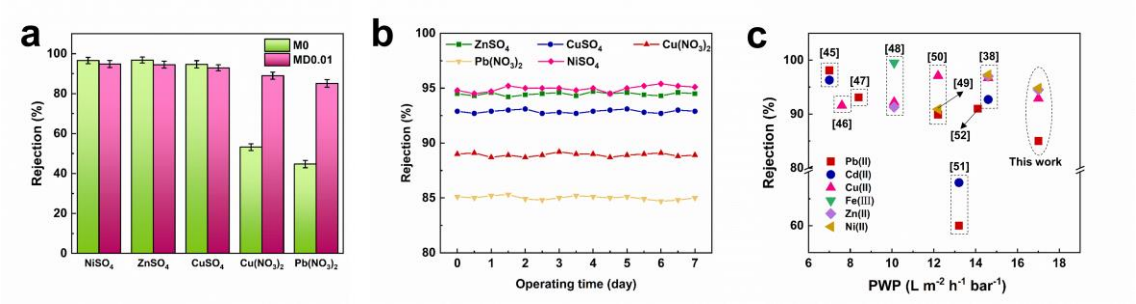

Fig. 10. (a) Rejection to different heavy metal salts of M0 and MD0.01 (2000 ppm, 25 ℃, 5.0 bar). (b) The rejection to heavy metals of MD0.01 in long term running (2000 ppm, 25 ℃, 5.0 bar). (c) The PWP and rejection to heavy metals of membranes in literature and this work [38, 45-52].

4. Conclusion

In conclusion, the dually charged PA NF membranes were facilely fabricated via microwave-assisted DETA modification after IP process. The modification constructed a positively charged layer on the negatively charged PA layer by introducing more amine groups, resulting in higher hydrophilicity and IEP. After grafting, the as-prepared membranes had a good PWP (17.0 L m^{-2} h^{-1} bar^{-1}) and high rejection to both Na_2SO_4 (98.2%) and $MgCl_2$ (94.1%), which cannot be achieved by the conventional negatively charged PA NF membranes. In addition, the dually charged NF membranes had high rejection to a series of heavy metals, showing application potential in heavy metals removal.

Acknowledgements

The financial support was provided by the National Natural Science Foundation of China (Grant No: 21808060), the Undergraduate Training Program for Innovation, and Entrepreneurship of East China University of Science and Technology (X20036).

References

[1] H. Borji, G.M. Ayoub, R. Bilbeisi, N. Nassar, L. Malaeb, How effective are nanomaterials for the removal of heavy metals from water and wastewater?, Water. Air. Soil. Pollu. 231 (2020) 330.

[2] L. Joseph, B.M. Jun, J.R.V. Flora, C.M. Park, Y. Yoon, Removal of heavy metals from water sources in the developing world using low-cost materials: A review, Chemosphere. 229 (2019) 142-159.

[3] M. Wołowiec, M. Komorowska-Kaufman, A. Pruss, G. Rzepa, T. Bajda, Removal of heavy metals and metalloids from water using drinking water treatment residuals as adsorbents: A review, Minerals. 9 (2019) 487.

[4] Z. Zia, A. Hartland, M.R. Mucalo, Use of low-cost biopolymers and biopolymeric composite systems for heavy metal removal from water, Int. J. Environ. Sci. Te. 17 (2020) 4389-4406.

[5] M. Hasanpour, M. Hatami, Application of three dimensional porous aerogels as adsorbent for removal of heavy metal ions from water/wastewater: A review study, Adv. Colloid. Interfac. 284 (2020) 102247.

[6] V.B. Yadav, R. Gadi, S. Kalra, Clay based nanocomposites for removal of heavy metals from water: A review, J. Environ. Manage. 232 (2019) 803-817.

[7] S. Wang, L. Li, S. Yu, B. Dong, N. Gao, X. Wang, A review of advances in EDCs and PhACs removal by nanofiltration: Mechanisms, impact factors and the influence of organic matter, Chem. Eng. J. 406 (2021) 126722.

[8] J. Lopez, M. Reig, X. Vecino, O. Gibert, J.L. Cortina, From nanofiltration membrane permeances to design projections for the remediation and valorisation of acid mine waters, Sci. Total. Environ. 738 (2020) 139780.

[9] M.A. Abdel-Fatah, Nanofiltration systems and applications in wastewater treatment: Review article, Ain. Shams. Eng. J. 9 (2018) 3077-3092.

[10] C.Z. Torma, E. Csefalvay, Nanofiltration: A final step in industrial process water treatment, Period. Polytech-Chem. 62 (2018) 68-75.

[11] C. H. Chu, C. Wang, H. F. Xiao, Q. Wang, W. J. Yang, N. Liu, X. Ju, J. X. Xie, S. P. Sun, Separation of ions with equivalent and similar molecular weights by nanofiltration: Sodium chloride and sodium acetate as an example, Sep. Purif. Technol. 250 (2020) 117199.

[12] B.Q. Huang, Y.J. Tang, Z.X. Zeng, Z.L. Xu, Microwave heating assistant preparation of high permselectivity polypiperazine-amide nanofiltration membrane during the interfacial polymerization process with low monomer concentration, J. Membr. Sci. 596 (2020) 117718.

[13] J.J. Wang, H.C. Yang, M.B. Wu, X. Zhang, Z.K. Xu, Nanofiltration membranes with cellulose nanocrystals as an interlayer for unprecedented performance, J. Mater. Chem. A. 5 (2017) 16289-16295.

[14] L. Cheng, M. Zhang, C. Fang, W. Feng, L. Zhu, Y. Xu, Positively charged poly (n-vinyl imidazole) gel-filled loose nanofiltration membranes: Performances and modelling analysis, J. Membr. Sci. 625 (2021) 118975.

[15] Q. Bi, C. Zhang, J. Liu, X. Liu, S. Xu, Positively charged zwitterion-carbon nitride functionalized nanofiltration membranes with excellent separation performance of Mg^{2+}/Li^{+} and good antifouling properties, Sep. Purif. Technol. 257 (2021) 117959.
[16] H. Z. Zhang, Z. L. Xu, H. Ding, Y. J. Tang, Positively charged capillary nanofiltration membrane with high rejection for Mg^{2+} and Ca^{2+} and good separation for Mg^{2+} and Li^{+}, Desalination. 420 (2017) 158-166.
[17] M. Peydayesh, T. Mohammadi, S.K. Nikouzad, A positively charged composite loose nanofiltration membrane for water purification from heavy metals, J. Membr. Sci. 611 (2020) 118205.
[18] Z. L. Qiu, W. H. Yu, Y. J. Shen, B. K. Zhu, L. F. Fang, Janus charged polyamide nanofilm with ultra-high separation selectivity for mono-/divalent ions, Chem. Eng. J. 416 (2021) 129023.
[19] S. Xu, D. Lu, P. Wang, Y. Zhao, Y. Sun, J. Qi, J. Ma, Polyphenol engineered membranes with dually charged sandwich structure for low-pressure molecular separation, J. Membr. Sci. 601 (2020) 117885.
[20] Y. Cao, H. Zhang, S. Guo, J. Luo, Y. Wan, A robust dually charged membrane prepared via catechol-amine chemistry for highly efficient dye/salt separation, J. Membr. Sci. 629 (2021) 119287.
[21] Y. Liang, S. Lin, Intercalation of zwitterionic surfactants dramatically enhances the performance of low-pressure nanofiltration membrane, J. Membr. Sci. 596 (2020) 117726.
[22] Y. Xiao, D. Guo, T. Li, Q. Zhou, L. Shen, R. Li, Y. Xu, H. Lin, Facile fabrication of superhydrophilic nanofiltration membranes via tannic acid and irons layer-by-layer self-assembly for dye separation, Appl. Surf. Sci. 515 (2020) 146063.
[23] S.H. Liu, C.R. Wu, W.S. Hung, X.L. Lu, K.R. Lee, One-step constructed ultrathin janus polyamide nanofilms with opposite charges for highly efficient nanofiltration, J. Mater. Chem. A. 5 (2017) 22988-22996.
[24] L. Yu, Y. Zhang, L. Xu, Q. Liu, B. Borjigin, D. Hou, J. Xiang, J. Wang, One step prepared janus acid-resistant nanofiltration membranes with opposite surface charges for acidic wastewater treatment, Sep. Purif. Technol. 250 (2020) 117245.
[25] X. Zhu, X. Cheng, J. Xing, T. Wang, D. Xu, L. Bai, X. Luo, W. Wang, G. Li, H. Liang, In-situ covalently bonded supramolecular-based protective layer for improving chlorine resistance of thin-film composite nanofiltration membranes, Desalination. 474 (2020) 114197.
[26] X. Yang, Y. Pu, Y. Zhang, X. Liu, J. Li, D. Yuan, X. Ning, Multifunctional composite membrane based on $BaTiO_3$@PU/PSA nanofibers for high-efficiency PM2.5 removal, J. Hazard. Mater. 391 (2020) 122254.
[27] B.Q. Huang, Y.J. Tang, Z. Zeng, S.M. Xue, C.H. Ji, Z.L. Xu, High-performance zwitterionic nanofiltration membranes fabricated via microwave-assisted grafting of betaine, ACS Appl. Mater. Inter. 12 (2020) 35523−35531.
[28] X. Zhang, T.H. Chen, F.F. Chen, H. Wu, C.Y. Yu, L.F. Liu, C.J. Gao, Structure adjustment for enhancing the water permeability and separation selectivity of the

thin film composite nanofiltration membrane based on a dendritic hyperbranched polymer, J. Membr. Sci. 618 (2021) 118455.
[29] X. Zhu, X. Tang, X. Luo, X. Cheng, D. Xu, Z. Gan, W. Wang, L. Bai, G. Li, H. Liang, Toward enhancing the separation and antifouling performance of thin-film composite nanofiltration membranes: A novel carbonate-based preoccupation strategy, J. Colloid. Interf. Sci. 571 (2020) 155-165.
[30] Y. Qian, H. Wu, S. P. Sun, W. Xing, Perfluoro-functionalized polyethyleneimine that enhances antifouling property of nanofiltration membranes, J. Membr. Sci. 611 (2020) 118286.
[31] J. Ding, H. Wu, P. Wu, Preparation of highly permeable loose nanofiltration membranes using sulfonated polyethylenimine for effective dye/salt fractionation, Chem. Eng. J. 396 (2020) 125199.
[32] A.J. Atkinson, J. Wang, Z. Zhang, A. Gold, D. Jung, D. Zeng, A. Pollard, O. Coronell, Grafting of bioactive 2-aminoimidazole into active layer makes commercial RO/NF membranes anti-biofouling, J. Membr. Sci. 556 (2018) 85-97.
[33] M. Zhou, J. Chen, W. Zhou, J. Sun, H. Tang, Developing composite nanofiltration membranes with highly stable antifouling property based on hydrophilic roughness, Sep. Purif. Technol. 256 (2021) 117799.
[34] J. Zhu, A. Uliana, J. Wang, S. Yuan, J. Li, M. Tian, K. Simoens, A. Volodin, J. Lin, K. Bernaerts, Y. Zhang, B. Van der Bruggen, Elevated salt transport of antimicrobial loose nanofiltration membranes enabled by copper nanoparticles via fast bioinspired deposition, J. Mater. Chem. A. 4 (2016) 13211-13222.
[35] Y.J. Tang, B.J. Shen, B.Q. Huang, Z.M. Zhan, Z.L. Xu, High permselectivity thin-film composite nanofiltration membranes with 3D microstructure fabricated by incorporation of beta cyclodextrin, Sep. Purif. Technol. 227 (2019) 115718.
[36] A. Bera, J.S. Trivedi, S.B. Kumar, A.K.S. Chandel, S. Haldar, S.K. Jewrajka, Anti-organic fouling and anti-biofouling poly(piperazineamide) thin film nanocomposite membranes for low pressure removal of heavy metal ions, J. Hazard. Mater. 343 (2018) 86-97.
[37] H.J. Zhang, B. Li, J.F. Pan, Y.W. Qi, J.N. Shen, C.J. Gao, B. Van der Bruggen, Carboxyl-functionalized graphene oxide polyamide nanofiltration membrane for desalination of dye solutions containing monovalent salt, J. Membr. Sci. 539 (2017) 128-137.
[38] J. Tian, H. Chang, S. Gao, R. Zhang, How to fabricate a negatively charged nf membrane for heavy metal removal via the interfacial polymerization between PIP and TMC?, Desalination. 491 (2020) 114499.
[39] L. Deng, S. Li, Y. Qin, L. Zhang, H. Chen, Z. Chang, Y. Hu, Fabrication of antifouling thin-film composite nanofiltration membrane via surface grafting of polyethyleneimine followed by zwitterionic modification, J. Membr. Sci. 619 (2021) 118564.
[40] K. Shen, P. Li, T. Zhang, X. Wang, Salt-tuned fabrication of novel polyamide composite nanofiltration membranes with three-dimensional turing structures for effective desalination, J. Membr. Sci. 607 (2020) 118153.

[41] C.R. Wu, S.H. Liu, Z.Y. Wang, J.H. Zhang, X. Wang, X.L. Lu, Y. Jia, W.S. Hung, K.R. Lee, Nanofiltration membranes with dually charged composite layer exhibiting super-high multivalent-salt rejection, J. Membr. Sci. 517 (2016) 64-72.
[42] B. Tansel, J. Sager, T. Rector, J. Garland, R.F. Strayer, L. Levine, M. Roberts, M. Hummerick, J. Bauer, Significance of hydrated radius and hydration shells on ionic permeability during nanofiltration in dead end and cross flow modes, Sep. Purif. Technol. 51 (2006) 40-47.
[43] Z. Liao, X. Fang, Q. Li, J. Xie, L. Ni, D. Wang, X. Sun, L. Wang, J. Li, Resorcinol-formaldehyde nanobowls modified thin film nanocomposite membrane with enhanced nanofiltration performance, J. Membr. Sci. 594 (2020) 117468.
[44] X. Zhu, D. Xu, Z. Gan, X. Luo, X. Tang, X. Cheng, L. Bai, G. Li, H. Liang, Improving chlorine resistance and separation performance of thin-film composite nanofiltration membranes with in-situ grafted melamine, Desalination. 489 (2020) 114539.
[45] S. Ibrahim, M. Mohammadi Ghaleni, A.M. Isloor, M. Bavarian, S. Nejati, Poly(homopiperazine-amide) thin-film composite membrane for nanofiltration of heavy metal ions, ACS Omega. 5 (2020) 28749-28759.
[46] S. Roy, S. Majumdar, G.C. Sahoo, S. Bhowmick, A.K. Kundu, P. Mondal, Removal of As(Ⅴ), Cr(Ⅵ) and Cu(Ⅱ) using novel amine functionalized composite nanofiltration membranes fabricated on ceramic tubular substrate, J Hazard. Mater. 399 (2020) 122841.
[47] K. Gu, S. Pang, B. Yang, Y. Ji, Y. Zhou, C. Gao, Polyethyleneimine/4,4′-bis(chloromethyl)-1,1′-biphenyl nanofiltration membrane for metal ions removal in acid wastewater, J. Membr. Sci. 614 (2020) 118497.
[48] X.Y. Gong, Z.H. Huang, H. Zhang, W.L. Liu, X.H. Ma, Z.L. Xu, C.Y. Tang, Novel high-flux positively charged composite membrane incorporating titanium-based MOFs for heavy metal removal, Chem. Eng. J. 398 (2020) 125706.
[49] W. Shao, C. Liu, T. Yu, Y. Xiong, Z. Hong, Q. Xie, Constructing positively charged thin-film nanocomposite nanofiltration membranes with enhanced performance, Polymers. 12 (2020).
[50] F. Mehrjo, A. Pourkhabbaz, A. Shahbazi, Pmo synthesized and functionalized by p-phenylenediamine as new nanofiller in pes-nanofiltration membrane matrix for efficient treatment of organic dye, heavy metal, and salts from wastewater, Chemosphere. 263 (2021) 128088.
[51] H. Z. Zhang, Z. L. Xu, J. Y. Sun, Three-channel capillary nf membrane with pamam-mwcnt-embedded inner polyamide skin layer for heavy metals removal, Rsc Advances. 8 (2018) 29455-29463.
[52] B.A.M. Al-Rashdi, D.J. Johnson, N. Hilal, Removal of heavy metal ions by nanofiltration, Desalination. 315 (2013) 2-17.

GRAPHIC ABSTRACT

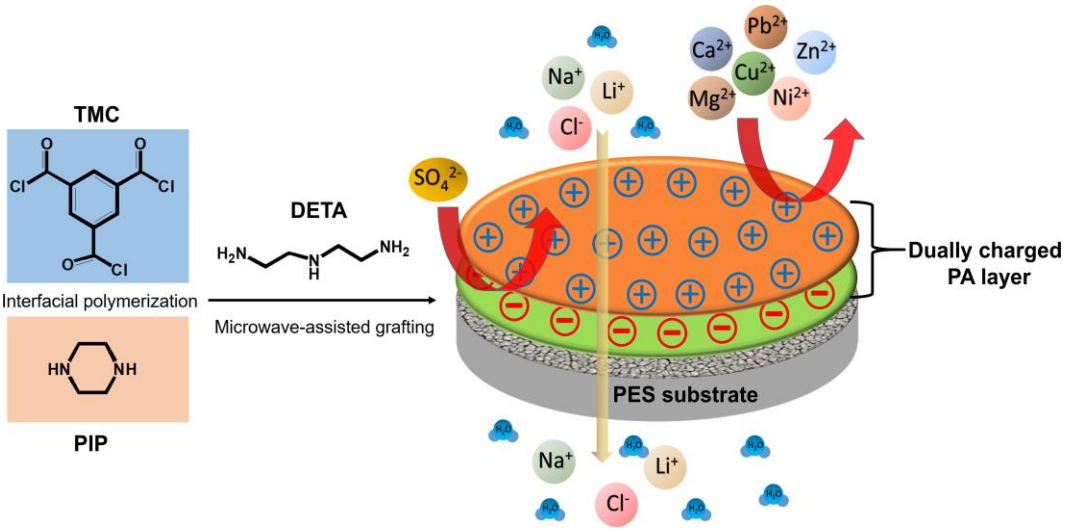

Fig. 1. Diagram and possible reactions of IP and DETA grafting process.

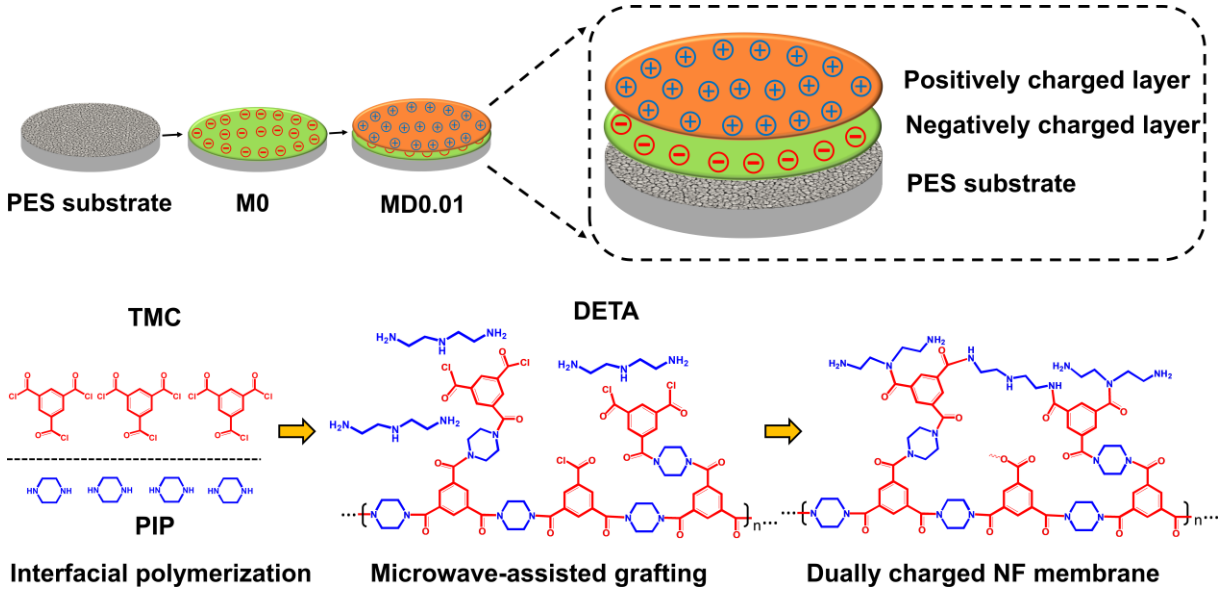

Fig. 2. FTIR spectra of NF membranes.

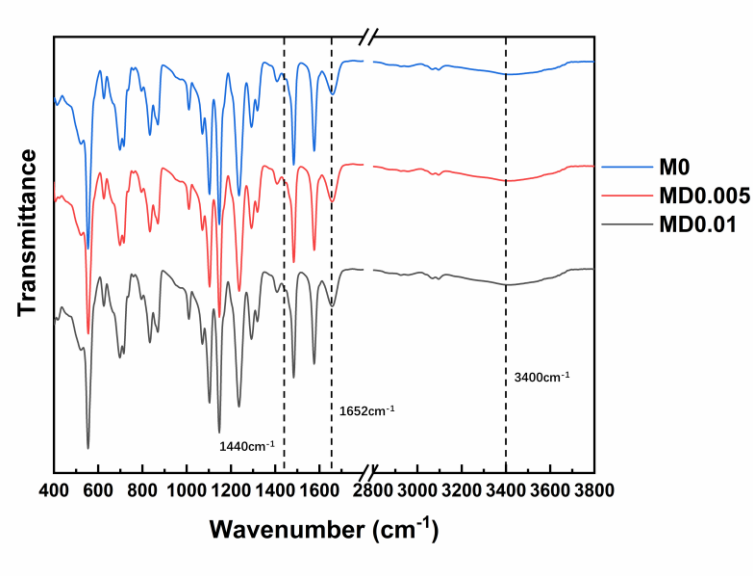

Fig. 3. (a) XPS spectra of PES UF substrate, M0, MD0.005, and MD0.01. C 1s spectra of (b) M0, (c) MD0.005, and (d) MD0.01.

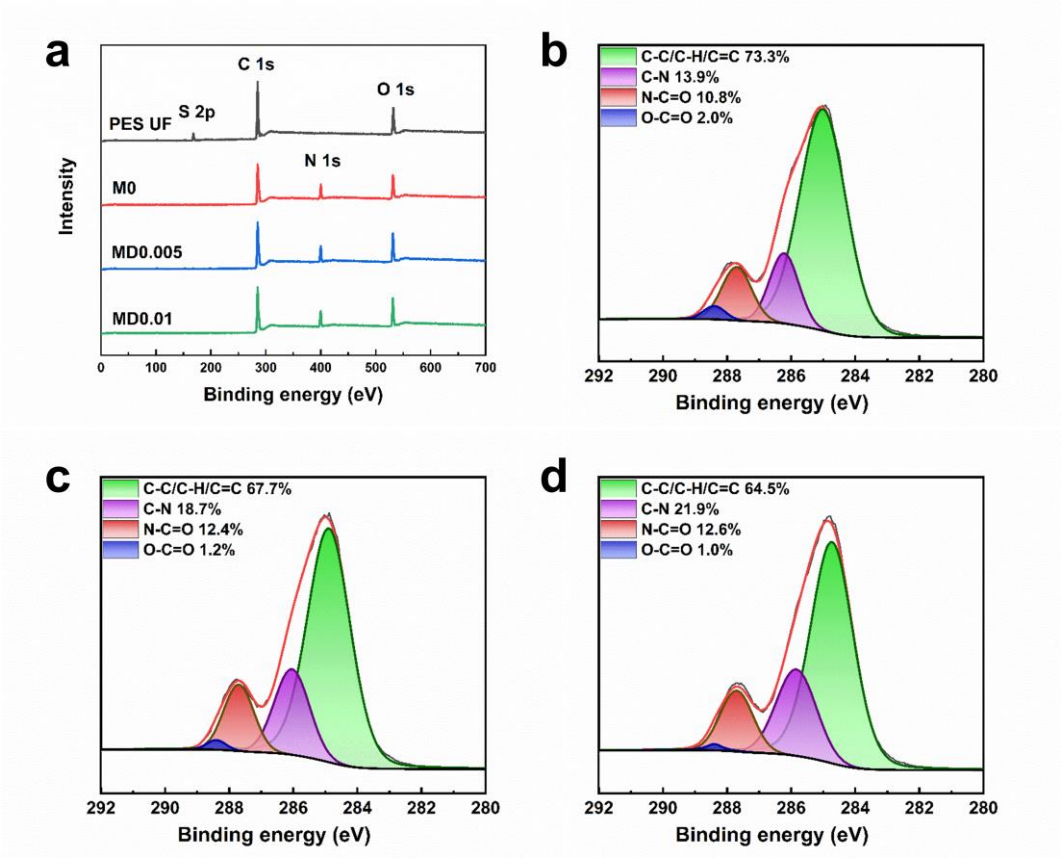

Fig. 4. SEM images of (a and e) PES UF substrate, (b and f) M0, (c and g) MD0.005, and (d and h) MD0.01.

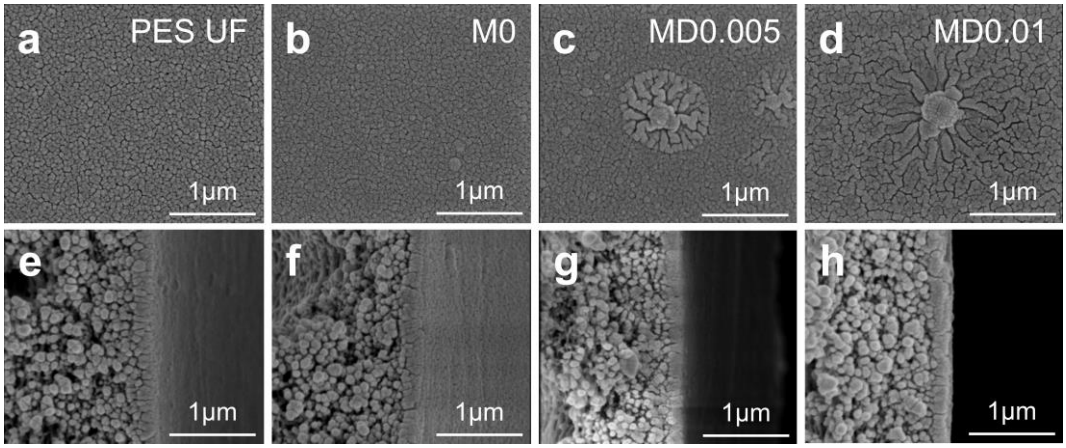

Fig. 5. AFM results of (a) PES UF substrate, (b) M0, (c) MD0.005, and (d) MD0.01 (testing area of 5μm×5μm).

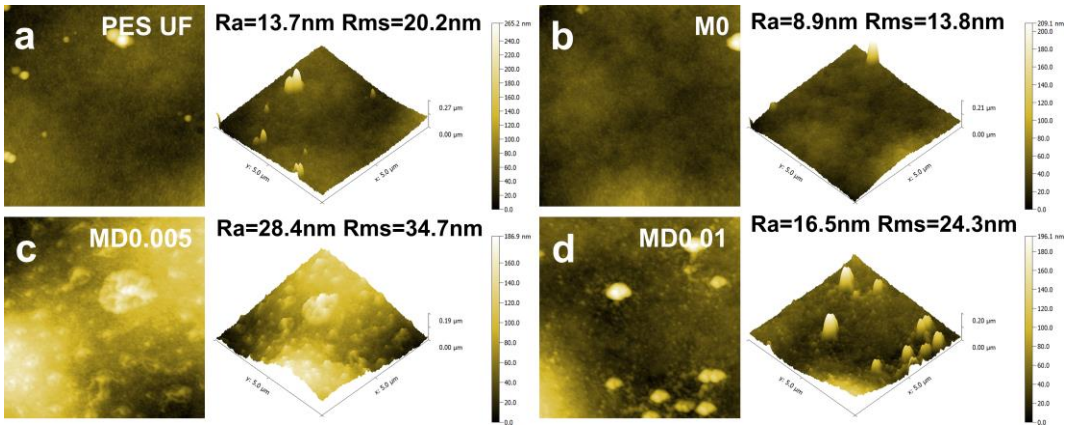

Fig. 6. (a) WCA of PES UF substrate, M0, MD0.005, and MD0.01. (b) Zeta potential of M0, MD0.005, and MD0.01 at pH value ranging of 4-10.

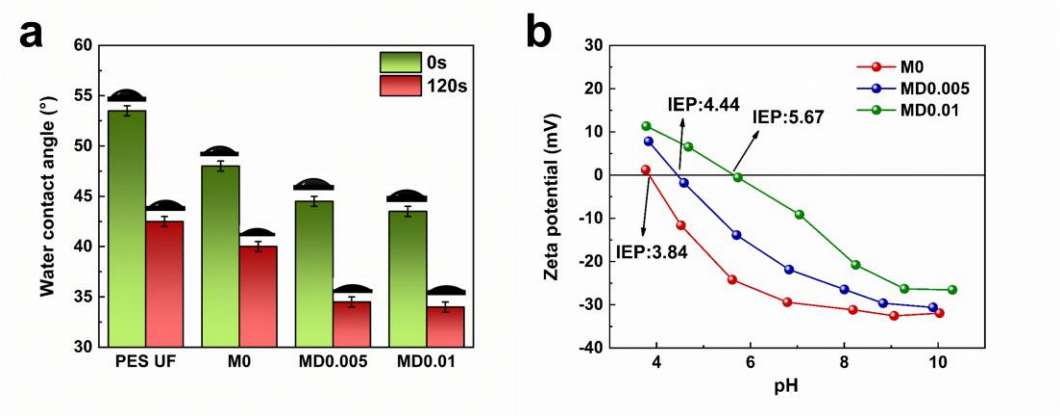

Fig. 7. (a) PWP and (b) Rejection to salts of M0 and membranes grafted with different concentrations of DETA (2000 ppm, 25 ℃, 5.0 bar).

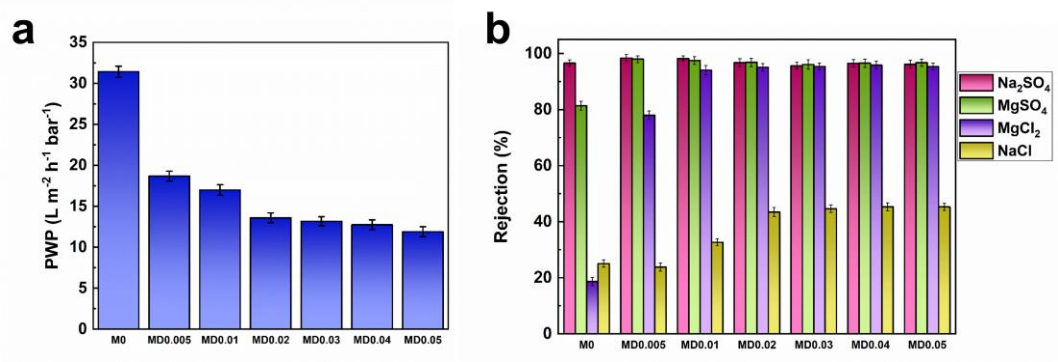

Fig. 8. Separation mechanism of the negatively and dually charged NF membranes.

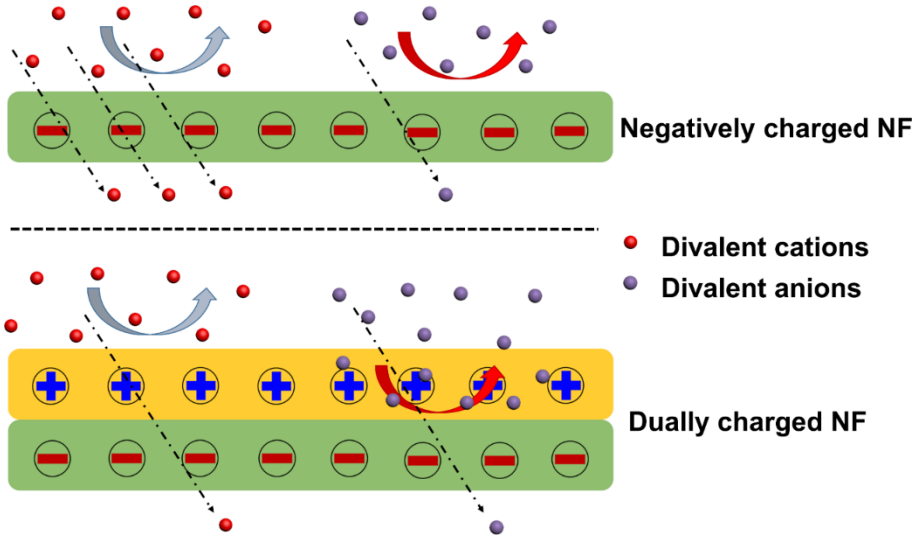

Fig. 9. (a) Rejection and permeability to different salts solution of MD0.01 (2000 ppm, 25 ℃, 5.0 bar). (b) Rejection to PEGs with different molecular weight of M0, MD0.005, and MD0.01 (300 ppm, 25 ℃, 5.0 bar).

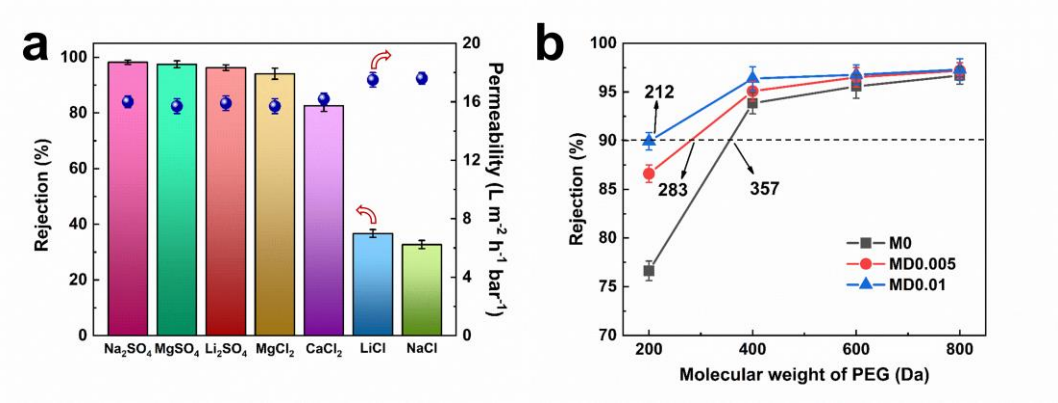

Fig. 10. (a) Rejection to different heavy metal salts of M0 and MD0.01 (2000 ppm, 25 ℃, 5.0 bar). (b) The rejection to heavy metals of MD0.01 in long term running (2000 ppm, 25 ℃, 5.0 bar). (c) The PWP and rejection to heavy metals of membranes in literature and this work [38, 45-52].

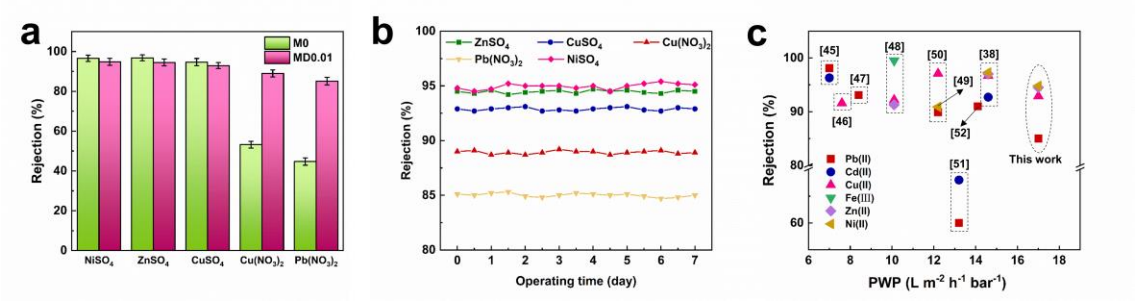

List of tables

Table 1 Elemental composition of PES UF substrate, M0, MD0.005, and MD0.01.

Sample	Atomic percent (%)				N/O ratio
	C 1s	N 1s	O 1s	S 2p	
PES UF	76.7±0.7	/	18.6±0.4	4.7±0.3	/
M0	71.1±1.0	12.1±0.5	16.8±0.5	/	0.72±0.05
MD0.005	69.5±0.9	13.5±0.4	17.0±0.4	/	0.79±0.04
MD0.01	69.8±1.1	13.9±0.5	16.3±0.4	/	0.85±0.05